Clinical Research Report

Journal of INTERNATIONAL MEDICAL RESEARCH

Journal of International Medical Research
2019, Vol. 47(3) 1210–1220

DOI: 10.1177/0300060518822406
journals.sagepub.com/home/imr
SAGE

Extranodal NK/T-cell lymphoma in adolescents: imaging findings of a consecutive 7-year case series

Pujun Guan[1,*], Zihang Chen[2,3,*], Lei Chu[1], Li Zhen[4], Li Zhang[3], Ling Pan[3], Weiping Liu[2] and Rongbo Liu[1]

Abstract

Objectives: Extranodal NK/T-cell lymphoma is reportedly a rare but emerging type of lymphoma in adolescents. The present study was performed to specify its imaging characteristics.

Methods: Our hospital's picture archiving and communication systems were searched from January 2009 to December 2016. We identified 13 patients aged <18 years with pathologically confirmed extranodal NK/T-cell lymphoma in the head and neck region. The computed tomography and magnetic resonance images were reviewed to summarize the imaging characteristics of extranodal NK/T-cell lymphoma in adolescents.

Results: The mean age at onset was 15.2 ± 1.46 years (range, 12–17 years) with a male:female ratio of 1.17:1.00. Most of the patients (n = 10) displayed nasal cavity and/or paranasal involvement. The tumor was homogeneous in both computed tomography and magnetic resonance images and showed slight enhancement. No calcification or liquefactive necrosis was observed. Adjacent structures were usually involved.

Conclusion: Suggestive imaging characteristics could acquaint specialists with extranodal NK/T-cell lymphoma in adolescents, facilitating improved early recognition of the diagnosis and helping to improve the patient's outcome.

[1]Department of Radiology, West China Hospital, Sichuan University, Chengdu, China
[2]Department of Pathology, West China Hospital, Sichuan University, Chengdu, China
[3]Department of Hematology, West China Hospital, Sichuan University, Chengdu, China
[4]Department of Operative Dentistry and Endodontics, West China Hospital of Stomatology, Sichuan University, Chengdu, China

*These authors contributed equally to this work.

Corresponding author:
Rongbo Liu, Department of Radiology, West China Hospital, Sichuan University, 37 Guo Xue Xiang, Chengdu, Sichuan 610041, China.
Email: cjr.liurongbo@vip.163.com

Keywords
Extranodal NK/T-cell lymphoma, adolescent, computed tomography, magnetic resonance imaging, imaging finding, tumor, diagnosis, head and neck, EBV, nose

Date received: 16 August 2018; accepted: 10 December 2018

Introduction

Extranodal NK/T-cell lymphoma (ENKTL) is an aggressive and rare tumor that is sporadic worldwide but more frequent in East Asia, Central, and South America.[1–6] Most affected patients are men in their 40s and 50s.[7–14] However, recent reports have indicated that among all patients with ENKTL, there is a small peak in the incidence at adolescence. ENKTL in adolescents is distinct from its counterpart in patients of advanced age in terms of its potentially closer association with aggressive NK-cell leukemia and chronic active Epstein–Barr virus (EBV) infection or other T/NK lymphoproliferative disorders.[15–18] However, little is known about ENKTL in adolescents.

Multiple imaging modalities have been widely used as effective screening tools for head and neck diseases. However, the radiological findings of ENKTL in adults are only occasionally reported, and to the best of our knowledge, no reports have focused on the imaging findings of ENKTL in adolescent patients.[19–24] The differences in the imaging features between ENKTL in adolescents and adults remain unclear. Furthermore, it is important for radiologists to understand this lymphoma type to enhance their differential diagnoses, especially given the large difference in the disease spectrum between aging adults and adolescents. Such knowledge could also help otolaryngologists, maxillofacial surgeons, and other specialists to avoid misdiagnosis. Therefore, in this consecutive 7-year case series, we summarized the computed tomography (CT) and magnetic resonance (MR) imaging findings of patients with ENKTL to reveal the imaging characteristics of ENKTL in adolescents.

Methods

Patients

Our hospital's picture archiving and communication systems were searched from January 2009 to December 2016. Consecutive patients aged <18 years who had pathologically confirmed ENKTL (based on the World Health Organization tumor classification) were included, and their clinical records were reviewed. Patients were excluded if their records did not include images of the primary lesions, CT or MR images, images before chemotherapy or radiotherapy, or lesions in the head and neck region. Basic patient information such as sex, age, symptoms, hemoglobin level, platelet count, lactate dehydrogenase (LDH) level in peripheral blood, and therapeutic regimens were extracted from the clinical records. Because this was a retrospective study and only limited information was disclosed, ethics approval was not necessary after consulting with the Ethics Committee of West China Hospital. Written informed consent was collected from all patients.

Imaging techniques and radiological analysis

CT scans were performed by one of the following scanners: Siemens SENSATION 16 (Siemens, Erlangen, Germany), Philips BRILLIANCE 64 (Philips Healthcare, Amsterdam, the Netherlands), Siemens SOMATOM Definition (Siemens), Siemens SOMATOM Definition AS (Siemens), or Siemens SOMATOM Definition FLASH (Siemens). Different protocols were applied according to the various disease sites and clinical practices. The scan ranges varied across different sites. MR imaging scans were performed by one of the following scanners: TOSHIBA EXCELART VANTAGE (1.5T) (Toshiba, Tokyo, Japan), Siemens Trio Tim (3.0T) (Siemens), or Siemens Sonata (1.5T) (Siemens). T1-weighted images (T1WI) and T2-weighted images (T2WI) were generated by two-dimensional sequences based on spin echo or fast/turbo spin echo sequences. At least two of three views (axial, sagittal, or coronal) were scanned. Fat saturation or fluid-attenuated inversion recovery was also applied to several selective sequences. Contrast-enhanced fat-suppressed images were obtained after intravenous injection of gadolinium-based agents.

Two radiologists analyzed the images independently before agreeing on a collective interpretation of the data together. The imaging parameters were the tumor position, necrosis, calcification, attenuation, degree of enhancement, enhancement pattern, local tumor invasion, lymphadenopathy, and metastasis. The enhancement pattern of the tumor was evaluated as homogeneous or heterogeneous. Local tumor invasion was defined as extension of the lesion into adjacent structures. Lymphadenopathy was assessed when at least one of the following features was present: enlargement (axial diameter of >10 mm in cervical and mesenteric areas), enhancement ring or irregular enhancement, and middle or irregular necrosis. Information on metastasis was mostly gathered from the clinical records except in cases of metastasis to organs within the scan areas and in cases in which CT or MR scans of other sites were performed at the same time. For MR images, T1WI, T2WI, and fluid-attenuated inversion recovery (FLAIR) signals were analyzed as augmentations. All signals were compared with normal skeletal muscles or as specifically mentioned below.

Pathological confirmation

All patients were diagnosed with ENKTL from samples obtained at biopsy. Pathological specimens were observed by hematoxylin–eosin staining and immunohistochemical staining. Standard immunohistochemical studies were performed using the following antibodies: CD20 (L26; Dako, Carpinteria, CA, USA), CD3 polyclonal (Polyclonal; Dako), CD5 (4C7; NeoMarkers, Fremont, CA, USA), CD56 (123C3; Zhongshan Bio-Tech, Zhongshan, China), Ki-67 (MIB-1; Dako), CD4 (1F6; Novocastra, Newcastle upon Tyne, UK), CD8 (C8; Dako), granzyme B (GZB01; NeoMarkers), and TIA-1 (2G910F5; Zhongshan Bio-Tech). EBV-encoded small RNA in situ hybridization (EBER-ISH) (No. Y520001; Dako) was performed to demonstrate the presence of EBV.

Results

Patients and clinical findings

Thirteen adolescents with ENKTL were included in this study (Table 1). Their mean age at onset was 15.2 ± 1.46 years (range, 12–17 years) with a male: female ratio of 1.17:1.00. More than half

Table 1. Clinical characteristics of 13 patients.

Variables	Number of patients (%)
Age, years	15.2 ± 1.46 (12–17)
Sex	
Male	7 (53.8)
Female	6 (46.2)
Symptoms	
Nasal obstruction	8 (61.5)
Fever	5 (38.5)
Par orbitalis edema	3 (23.1)
Facial edema	3 (23.1)
Purulent nasal discharge	3 (23.1)
Anemia	
Yes	3 (23.1)
No	10 (76.9)
Thrombocytopenia	
Yes	3 (23.1)
No	10 (76.9)
Elevated LDH	
Yes	4 (30.8)
No	9 (69.2)
Treatment	
Chemotherapy	6 (66.7)
Chemotherapy + radiotherapy	1 (11.1)
Chemotherapy + HSCT	1 (11.1)
No treatment	1 (11.1)

Age is presented as mean ± standard deviation (range). LDH, lactate dehydrogenase; chemotherapy, all chemotherapeutic regimens were L-asparaginase-based regimens; HSCT, hematopoietic stem cell transplantation.

of the patients (n = 7) had nasal obstructions, while three patients had purulent nasal discharge. Three patients had facial edema, two patients had pars orbitalis edema, and three patients had fevers. Each patient had only head and neck involvement, even those with advanced-stage cancer (stage III/IV). With respect to the laboratory findings, three patients were diagnosed with anemia, three patients were diagnosed with thrombocytopenia, and two patients had an elevated LDH level. Most of the patients (n = 9) received chemotherapy with an L-asparaginase-based regimen. The detailed information regarding the clinical findings are summarized in the supplementary data provided in Table S1.

Radiological findings

Among the 13 adolescents with ENKTL, 12 underwent CT scans, 3 underwent MR imaging, and only 2 underwent both MR imaging and CT scans. Five patients underwent contrast-enhanced scans (CT, n = 3; MR imaging, n = 3). The slice thickness of the CT scans was <3 mm in 11 of the patients and multiplanar-reconstructed in three views. The slice thickness of the one other patient's images was 9 mm for screening of intracranial abnormities because his chief complaint was a 17-day history of failing eyesight in the left eye. Later, MR imaging was performed and used to evaluate the lesion in the nose region.

The tumor sites and characteristics of local tumor invasion among all 13 patients were as follows. Ten patients showed nasal cavity and/or paranasal involvement, and three patients mainly showed nasopharynx involvement. Lymphadenopathy was seen in most of the patients (n = 9); however, because of the limited images, no systematic investigation was performed. On the basis of the medical records and imaging materials, one patient had a mediastinal mass that was considered to be metastasis.

Among the 10 patients with nasal and/or paranasal involvement (Figure 1), 8 patients had lesions on both sides of the nasal cavity. Among these eight patients, one patient's tumor was dominant in the left nasal cavity with asymmetrical thickening and destruction of the nasal septum; it also occupied the inferior nasal meatus. The other seven patients had obvious lesions on both sides of the nasal cavity. These eight patients' lesions were also found in the maxillary sinus (left, n = 3; right, n = 1; bilateral, n = 2), the anterior ethmoid sinus (bilateral, n = 6), the frontal sinus (left, n = 1; right, n = 2; bilateral, n = 1), the posterior ethmoid sinus (left, n = 1; right, n = 1; bilateral, n = 4), the sphenoid sinus (right, n = 2; bilateral,

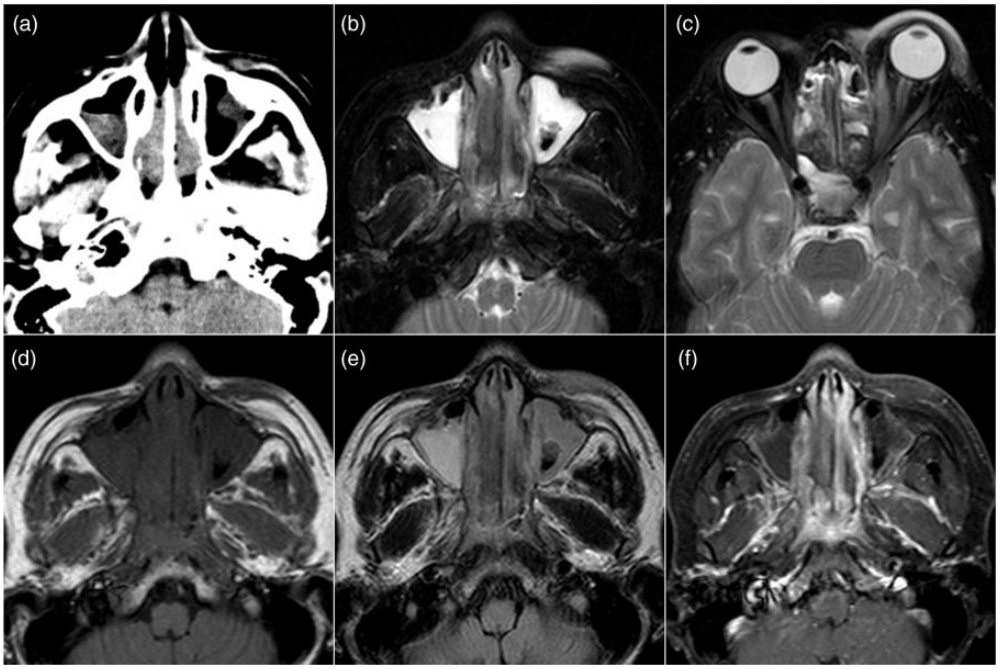

Figure 1. A 15-year-old male patient presented with a 17-day history of failing eyesight in the left eye. (a) Computed tomography images of the nasal lesion. (b, d, e, f) Magnetic resonance images of the nasal lesion (b, T2-weighted imaging; d, T1-weighted imaging; e, fluid-attenuated inversion recovery; f, contrast enhancement). (c) T2-weighted imaging shows edema of the left eyelid, enlargement of the right medial rectus muscle, and displacement and compression of the optic nerve.

n = 2), the extraconal orbital space (left, n = 2; right, n = 1), the intraconal orbital space (left, n = 1; right, n = 1), the soft palate (n = 4), the hard palate (n = 3), the nasopharynx (n = 2), the nasal septum (n = 7), the nasal ala (n = 4), and the facial skin and subcutaneous tissue (n = 3). The remaining 2 of the 13 patients, whose major involvement was in the facial soft tissue (unilateral, n = 1; bilateral, n = 1), had lesions in the nasal septa and/or turbinates (Figure 2).

All three patients with nasopharyngeal involvement (Figure 3) showed large exophytic nasopharyngeal masses occupying a majority of the airway and invading the surrounding fascial spaces and tissues. In all three patients, the tumors invaded the choanae, stretching along with the turbinates and involving the prevertebral spaces, the parapharyngeal spaces of both sides, and the soft and hard palates; they then extended to the oropharynx and involved Waldeyer's ring. Among these three patients, two had tumors that invaded the left pterygopalatine fossa and the posterior ethmoid sinus, one of whom also had lesions in the maxillary sinuses. The other patient's tumor invaded the posterior ethmoid sinus and the sphenoid sinus of the right side.

At all sites, the tumors ranged from an infiltrative pattern to a mass-forming pattern. In the CT images, the lesions in the nasal or nasopharyngeal areas were homogeneous (similar to normal muscles) in most cases (10 of 12 cases; 2 cases were slightly heterogeneous). Among these 12 tumors,

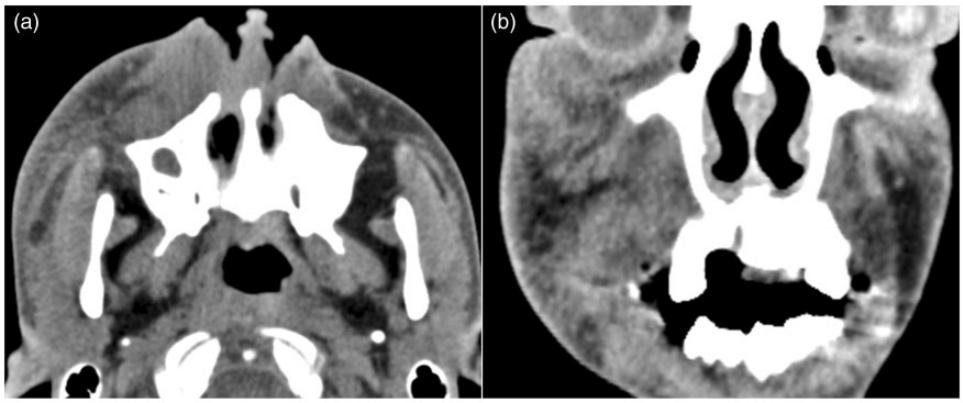

Figure 2. A 16-year-old male patient presented with a 1-month history of right facial edema. (a, b) Computed tomography images of the mass beneath the skin.

Figure 3. A 14-year-old female patient presented with a 7-day history of bilateral nasal obstruction and pharyngalgia and a 3-day history of fever. (a, b) Computed tomography images of the pharyngeal lesion (b, contrast-enhanced scan).

most were isodense compared with the normal skeletal muscles (n = 9); some also had small patches that were isodense to gray matter (n = 3). In the nasal cavities, slightly hypodense or isodense areas (compared with the white matter) could usually be found on the verge of a hyperdense lesion, which may reflect inflammation around the tumor (8 of 10 cases). The patients had severe swelling when the tumor involved the facial skin and subcutaneous tissue (3 of 3 cases). No calcification was observed in any of these cases. In the MR images, the tumors showed homogeneous isointensity in T1WI and slight hyperintensity in T2WI (3 of 3 cases). FLAIR images could distinguish between the tumor and inflammatory mucosa.

No liquefactive necrosis was found. The tumor exhibited slight homogeneous enhancement, although to a lesser degree than that of the mucosa.

Pathological findings

In most patients, the tumors showed extensive necrosis with an angiocentric pattern. The tumor cells were positive for CD3 polyclonal, CD56, and granzyme B or TIA-1 and negative for CD20, CD5, CD4, and CD8. The result of EBER-ISH was positive for all cases. The rate of Ki-67 positivity ranged from 30% to 90%.

Discussion

Theoretically, people of all ages could be susceptible to ENKTL, but the literature regarding ENKTL in adolescents is very sparse.[15–18] No reports provide imaging characteristics regarding ENKTL in adolescents. To the best of our knowledge, this is the first empirical record of the imaging findings of ENKTL in this patient population. We have provided a systematic descriptive analysis of the imaging features. No clear differences in the imaging findings were found between ENTKL in adolescents and adults. However, this empirical record provides evidence that this disease should be considered as a differential diagnosis. When ENKTL occurs in adolescents, it usually progresses rapidly, similar to aggressive NK-cell leukemia. However, early-stage ENKTL in adolescents may respond well to radiotherapy.[25] Therefore, it is important for radiologists to be aware of the indicative characteristics of ENKTL to recognize patients with probable ENKTL and recommend an endoscopic biopsy to avoid treatment delay.

From a clinical standpoint, symptoms related to the upper aerodigestive tract, especially the nasal cavities, are common among both adults and adolescents with ENKTL.[26] In the present study, 80% of the patients with ENKTL had nasal involvement in the form of nasal obstruction and rhinorrhea, similar to prior studies of adults with ENKTL.[27,28] Moreover, the proportion of adolescent patients with ENKTL who had orbital symptoms was significantly higher than that of adult patients with ENKTL ($p = 0.041$); this may have been due to the patients' undeveloped bone structures and immune system.[29] Additionally, adolescent patients are more likely to present with facial edema ($p = 0.001$) but are less likely to have epistaxis ($p = 0.011$) compared with adult patients (supplementary data, Table S2). With respect to laboratory testing, both adult and adolescent patients with ENKTL shared similar changes in routine blood tests, with only a minority of patients (<30%) exhibiting anemia and/or thrombocytopenia. However, fewer adolescent than adult patients with ENKTL had an elevated LDH level.[27] This finding indicates that clinicians should not neglect adolescent patients with upper aerodigestive tract symptoms and a normal LDH level.

The nasal and/or paranasal areas are the most common sites of ENKTL in adolescents. The imaging features are not specific for ENKTL, but they are suggestive. The lesions are always on both sides of the nasal cavity with involvement of the septa, turbinates, and drainage pathways of the paranasal sinus (most often the ethmoid sinus and maxillary sinus). Obstructed drainage pathways may be associated with the development of acute inflammation or retention cysts around the tumor. Involvement of the facial soft tissues is less common and is always characterized by severe facial edema. The tumor is homogeneous in both CT and MR images and shows slight enhancement. No liquefactive necrosis or calcification was observed in the present study. Clinical features such as B symptoms and an elevated LDH level

must also be taken into consideration. Therefore, an endoscopic biopsy is recommended when some of these characteristics are present in adolescent patients.

To obtain a correct diagnosis of lesions in the nasal cavity and nasopharyngeal region, the site and the morphology need to be carefully analyzed. Other radiological characteristics such as the signal intensity, attenuation, enhancement characteristics, clinical features, and endoscopy findings should also be taken into consideration.[30,31] Some tumors and tumor-like lesions of the nasal cavity, paranasal sinus, and nasopharyngeal region have classic locations and morphological characteristics, such as juvenile nasal angiofibroma, mucocele, antrochoanal polyp, fungal infection, and many congenital and developmental abnormalities.[30] Inflammation may be observed, but the diagnostic clues for tumors must be carefully investigated (such as different attenuation and enhancement patterns) to avoid inaccurate diagnoses.

Differential diagnoses are often extremely difficult to make.[32] The differential diagnosis between reactive lymphoid hyperplasia and lymphoma is very difficult because these two conditions share many histological similarities. Some studies suggest that enhanced MR imaging may better distinguish reactive lymphoid hyperplasia.[33,34] To identify various types of lymphoma, the biological characteristics of lymphoma (indolent, aggressive, or highly aggressive), primary site (nodal or extranodal, anatomical regions), systemic involvement (hepatosplenomegaly, multiple lymphadenopathy, leukemic appearance, cutaneous involvement, or bone marrow invasion), and endemicity (e.g., Burkitt lymphoma is endemic in Africa and is characterized by a jaw mass, while gastrointestinal tract lymphoma is endemic in China) could be helpful for obtaining an imaging diagnosis; however, a biopsy is still required for confirmation. Other difficult differential diagnoses are granulomatous diseases, such as tuberculosis. Although nasal tuberculosis is rare, it is quite difficult to distinguish ENKTL from tuberculosis through radiological features if no calcification occurs, even by hematoxylin–eosin staining.[35] Other rare diseases that can occur in this area in children and adolescents include rhabdomyosarcoma,[36] Langerhans cell histiocytosis,[37] Rosai–Dorfman disease,[38,39] central giant cell granuloma,[40] sinonasal carcinoma,[41] fibrosarcoma, synovial sarcoma, osteosarcoma,[42] and nasopharyngeal carcinoma.[43] Pathologists often have difficulty diagnosing these diseases. Thus, the role of radiologists is to recognize the possible diagnostic spectrum on an individual-patient basis, ensure consistency with imaging findings, and recommend a biopsy when necessary.

Several studies have investigated the prognostic value of imaging findings. Primary tumor invasion in both MR imaging and CT has been demonstrated to be a risk factor.[20,24] Additionally, detection of a mass-forming pattern and cervical lymphadenopathy in CT images indicates worse overall survival of patients with early-stage (stage I/II) ENKTL.[20] More work should be done to evaluate the prognostic value of imaging findings of adolescent patients with ENKTL in comparison with adults with ENKTL.

This retrospective study was based on inpatient cases in our hospital. The major limitation is that we could not apply quantifiable methods and obtain more homogeneous multimodality-imaging information. To some extent, this reflects the poor understanding of this rare type of lymphoma. CT is helpful for evaluating bones and planning partial turbinate resection to relieve symptoms. MR imaging, especially enhanced MR imaging, is essential not only for evaluating the mass itself but also for measuring the surrounding structures. In addition, MR imaging is a better choice than CT

for children and adolescents considering the dangers of ionizing radiation. New technologies such as diffusion-based MR imaging, perfusion-based MR imaging, MR fingerprints, quantitative MR imaging, MR spectroscopy, and molecular imaging need to be further studied to help diagnose and understand these diseases more thoroughly.

Conclusions

The radiological features of ENKTL in adolescents are not specific. The suggestive features include location, local involvement, signal intensity or attenuation, and enhancement. No calcification or liquefactive necrosis should be present. If classic radiological features are observed, especially alongside clinical symptoms and anomalies in laboratory testing, a biopsy should be recommended to avoid delays in treatment and to improve the patient's outcome.

Acknowledgements

We thank Corey Hu for assisting with the study. We also appreciate all of the patients and their guardians who were involved in this study and extend our best wishes to them.

Authors' contributions

GPJ collected the radiological information and drafted the main parts of the manuscript. GPJ and LRB interpreted the images. CZH collected the pathological and clinical information and drafted relevant parts of the manuscript. CZH, Zhen L, CL LRB, Zhang L, and PL revised the paper. All authors read and approved the final manuscript.

Availability of data and materials

The datasets analyzed during the current study are available from the corresponding author on reasonable request with ethical approval.

Declaration of conflicting interest

The authors declare that there is no conflict of interest.

Funding

This research received no specific grant from any funding agency in the public, commercial, or not-for-profit sectors.

ORCID iD

Pujun Guan http://orcid.org/0000-0002-7288-9369

References

1. Laurini JA, Perry AM, Boilesen E, et al. Classification of non-Hodgkin lymphoma in Central and South America: a review of 1028 cases. *Blood* 2012; 120: 4795–4801.
2. The world health organization classification of malignant lymphomas in Japan: incidence of recently recognized entities. Lymphoma Study Group of Japanese Pathologists. *Pathol Int* 2000; 50: 696–702.
3. Quintanilla-Martinez L, Franklin JL, Guerrero I, et al. Histological and immunophenotypic profile of nasal NK/T cell lymphomas from Peru: high prevalence of p53 overexpression. *Hum Pathol* 1999; 30: 849–855.
4. Au WY, Ma SY, Chim CS, et al. Clinicopathologic features and treatment outcome of mature T-cell and natural killer-cell lymphomas diagnosed according to the World Health Organization classification scheme: a single center experience of 10 years. *Ann Oncol* 2005; 16: 206–214.
5. Chen Z, Guan P, Shan T, et al. CD30 expression and survival in extranodal NK/T-cell lymphoma: a systematic review and meta-analysis. *Oncotarget* 2018; 9: 16547–16556.
6. Yang QP, Zhang WY, Yu JB, et al. Subtype distribution of lymphomas in Southwest China: analysis of 6,382 cases using WHO classification in a single institution. *Diagn Pathol* 2011; 6: 77.
7. Au WY, Weisenburger DD, Intragumtornchai T, et al. Clinical differences between nasal and extranasal natural killer/T-cell lymphoma: a study of 136 cases from the International Peripheral T-Cell Lymphoma Project. *Blood* 2009; 113: 3931–3937.

8. Chan JK, Sin VC, Wong KF, et al. Nonnasal lymphoma expressing the natural killer cell marker CD56: a clinicopathologic study of 49 cases of an uncommon aggressive neoplasm. *Blood* 1997; 89: 4501–4513.
9. Cheung MM, Chan JK, Lau WH, et al. Primary non-Hodgkin's lymphoma of the nose and nasopharynx: clinical features, tumor immunophenotype, and treatment outcome in 113 patients. *J Clin Oncol* 1998; 16: 70–77.
10. Gualco G, Domeny-Duarte P, Chioato L, et al. Clinicopathologic and molecular features of 122 Brazilian cases of nodal and extranodal NK/T-cell lymphoma, nasal type, with EBV subtyping analysis. *Am J Surg Pathol* 2011; 35: 1195–1203.
11. Jhuang JY, Chang ST, Weng SF, et al. Extranodal natural killer/T-cell lymphoma, nasal type in Taiwan: a relatively higher frequency of T-cell lineage and poor survival for extranasal tumors. *Hum Pathol* 2015; 46: 313–321.
12. Li S, Feng X, Li T, et al. Extranodal NK/T-cell lymphoma, nasal type: a report of 73 cases at MD Anderson Cancer Center. *Am J Surg Pathol* 2013; 37: 14–23.
13. Park S and Ko YH. Epstein-Barr virus-associated T/natural killer-cell lymphoproliferative disorders. *J Dermatol* 2014; 41: 29–39.
14. Pongpruttipan T, Sukpanichnant S, Assanasen T, et al. Extranodal NK/T-cell lymphoma, nasal type, includes cases of natural killer cell and alphabeta, gammadelta, and alphabeta/gammadelta T-cell origin: a comprehensive clinicopathologic and phenotypic study. *Am J Surg Pathol* 2012; 36: 481–499.
15. Huang Y, Xie J, Ding Y, et al. Extranodal natural killer/T-cell lymphoma in children and adolescents: a report of 17 cases in China. *Am J Clin Pathol* 2016; 145: 46–54.
16. Hutchison RE, Laver JH, Chang M, et al. Non-anaplastic peripheral t-cell lymphoma in childhood and adolescence: a Children's Oncology Group study. *Pediatr Blood Cancer* 2008; 51: 29–33.
17. Ohshima K, Kimura H, Yoshino T, et al. Proposed categorization of pathological states of EBV-associated T/natural killer-cell lymphoproliferative disorder (LPD) in children and young adults: overlap with chronic active EBV infection and infantile fulminant EBV T-LPD. *Pathol Int* 2008; 58: 209–217.
18. Rodriguez-Pinilla SM, Barrionuevo C, Garcia J, et al. EBV-associated cutaneous NK/T-cell lymphoma: review of a series of 14 cases from Peru in children and young adults. *Am J Surg Pathol* 2010; 34: 1773–1782.
19. Hung LY, Chang PH, Lee TJ, et al. Extranodal natural killer/T-cell lymphoma, nasal type: clinical and computed tomography findings in the head and neck region. *Laryngoscope* 2012; 122: 2632–2639.
20. Kim JY, Lee SW, Lee JH, et al. Stage IE/IIE extranodal NK/T-cell lymphoma arising in the nasal cavity: analysis of CT findings and their prognostic value. *Clin Radiol* 2013; 68: e384–e390.
21. King AD, Lei KI, Ahuja AT, et al. MR imaging of nasal T-cell/natural killer cell lymphoma. *AJR Am J Roentgenol* 2000; 174: 209–211.
22. Ooi GC, Chim CS, Liang R, et al. Nasal T-cell/natural killer cell lymphoma: CT and MR imaging features of a new clinicopathologic entity. *AJR Am J Roentgenol* 2000; 174: 1141–1145.
23. Ou CH, Chen CC, Ling JC, et al. Nasal NK/T-cell lymphoma: computed tomography and magnetic resonance imaging findings. *J Chin Med Assoc* 2007; 70: 207–212.
24. Wu RY, Liu K, Wang WH, et al. Patterns of primary tumor invasion and regional lymph node spread based on magnetic resonance imaging in early-stage nasal NK/T-cell lymphoma: implications for clinical target volume definition and prognostic significance. *Int J Radiat Oncol Biol Phys* 2017; 97: 50–59.
25. Wang ZY, Li YX, Wang WH, et al. Primary radiotherapy showed favorable outcome in treating extranodal nasal-type NK/T-cell lymphoma in children and adolescents. *Blood* 2009; 114: 4771–4776.
26. Wu X, Li P, Zhao J, et al. A clinical study of 115 patients with extranodal natural killer/T-cell lymphoma, nasal type. *Clin Oncol (R Coll Radiol)* 2008; 20: 619–625.

27. Haverkos BM, Pan Z, Gru AA, et al. Extranodal NK/T cell lymphoma, nasal type (ENKTL-NT): an update on epidemiology, clinical presentation, and natural history in North American and European cases. *Curr Hematol Malig Rep* 2016; 11: 514–527.
28. Kim SJ, Yoon DH, Jaccard A, et al. A prognostic index for natural killer cell lymphoma after non-anthracycline-based treatment: a multicentre, retrospective analysis. *Lancet Oncol* 2016; 17: 389–400.
29. Jimenez-Perez JC and Yoon MK. Natural killer T-cell lymphoma of the orbit: an evidence-based approach. *Semin Ophthalmol* 2017; 32: 116–124.
30. Rodriguez DP, Orscheln ES and Koch BL. Masses of the nose, nasal cavity, and nasopharynx in children. *Radiographics* 2017; 37: 1704–1730.
31. Bohman L, Mancuso A, Thompson J, et al. CT approach to benign nasopharyngeal masses. *AJR Am J Roentgenol* 1981; 136: 173–180.
32. Holsinger FC, Hafemeister AC, Hicks MJ, et al. Differential diagnosis of pediatric tumors of the nasal cavity and paranasal sinuses: a 45-year multi-institutional review. *Ear Nose Throat J* 2010; 89: 534–540.
33. Westacott S, Garner A, Moseley IF, et al. Orbital lymphoma versus reactive lymphoid hyperplasia: an analysis of the use of computed tomography in differential diagnosis. *Br J Ophthalmol* 1991; 75: 722–725.
34. Akansel G, Hendrix L, Erickson BA, et al. MRI patterns in orbital malignant lymphoma and atypical lymphocytic infiltrates. *Eur J Radiol* 2005; 53: 175–181.
35. Moon WK, Han MH, Chang KH, et al. CT and MR imaging of head and neck tuberculosis. *Radiographics* 1997; 17: 391–402.
36. Haussler SM, Stromberger C, Olze H, et al. Head and neck rhabdomyosarcoma in children: a 20-year retrospective study at a tertiary referral center. *J Cancer Res Clin Oncol* 2018; 144: 371–379.
37. Chevallier KM, Wiggins RH, Quinn NA, et al. Differentiating pediatric rhabdomyosarcoma and langerhans cell histiocytosis of the temporal bone by imaging appearance. *AJNR Am J Neuroradiol* 2016; 37: 1185–1189.
38. Zaveri J, La Q, Yarmish G, et al. More than just langerhans cell histiocytosis: a radiologic review of histiocytic disorders. *Radiographics* 2014; 34: 2008–2024.
39. Raslan OA, Schellingerhout D, Fuller GN, et al. Rosai-Dorfman disease in neuroradiology: imaging findings in a series of 10 patients. *AJR Am J Roentgenol* 2011; 196: W187–W193.
40. Seo ST, Kwon KR, Rha KS, et al. Pediatric aggressive giant cell granuloma of nasal cavity. *Int J Surg Case Rep* 2015; 16: 67–70.
41. Robson CD, Rahbar R, Vargas SO, et al. Sinonasal and laryngeal carcinoma in children: correlation of imaging characteristics with clinicopathologic and cytogenetic features. *AJNR Am J Neuroradiol* 2010; 31: 257–261.
42. Koka V, Vericel R, Lartigau E, et al. Sarcomas of nasal cavity and paranasal sinuses: chondrosarcoma, osteosarcoma and fibrosarcoma. *J Laryngol Otol* 1994; 108: 947–953.
43. Bass IS, Haller JO, Berdon WE, et al. Nasopharyngeal carcinoma: clinical and radiographic findings in children. *Radiology* 1985; 156: 651–654.